Mon. Not. R. Astron. Soc. **000**, 1–?? (2008) Printed 20 November 2014 (MN LATEX style file v2.2)

Metal loading of giant gas planets

Sergei Nayakshin
Department of Physics & Astronomy, University of Leicester, Leicester, LE1 7RH, UK
E-mail: Sergei.Nayakshin@le.ac.uk

arXiv:1411.5261v1 [astro-ph.EP] 19 Nov 2014

Received

ABSTRACT

One of many challenges in forming giant gas planets via Gravitational disc Instability model (GI) is an inefficient radiative cooling of the pre-collapse fragments. Since fragment contraction times are as long at $10^5 - 10^7$ years, the fragments may be tidally destroyed sooner than they contract into gas giant planets. Here we explore the role of "pebble accretion" onto the pre-collapse giant planets and find an unexpected result. Despite larger dust opacity at higher metallicities, addition of metals actually accelerates – rather than slows down – collapse of high opacity, relatively low mass giant gas planets ($M_p \lesssim$ a few Jupiter masses). A simple analytical theory that explains this result exactly in idealised simplified cases is presented. The theory shows that planets with the central temperature in the range of $1000 \lesssim T_{\rm c} \lesssim 2000$ K are especially sensitive to pebble accretion: addition of just ~ 5 to 10% of metals by weight is sufficient to cause their collapse. These results show that dust grain physics and dynamics is essential for an accurate modelling of self-gravitating disc fragments and their near environments in the outer massive and cold protoplanetary discs.

1 INTRODUCTION AND BACKGROUND

Gravitational disc Instability (GI) theory for giant planet formation (e.g., Kuiper 1951; Cameron et al. 1982; Boss 1997, 1998) posits that gravitational instability of the disc leads to formation of self-gravitating gas fragments that later contract into present day planets. This view has been strongly challenged in the last decade since it was shown that protoplanetary discs do not cool rapidly enough to fragment onto gas clumps inside several tens to a hundred AU (Gammie 2001; Mayer et al. 2004; Rice et al. 2005; Rafikov 2005; Durisen et al. 2007; Stamatellos & Whitworth 2008; Meru & Bate 2011). This would preclude the model from explaining most of the giant planets, since most are detected at separations much smaller than this, all the way down to ~ 0.05 AU (e.g., Mayor & Queloz 1995).

However, Nayakshin (2010a) argued that giant planets could be born far out but then migrate inward arbitrarily close to the parent star due to gravitational torques of the disc (e.g., Lin & Papaloizou 1979; Goldreich & Tremaine 1980). Crucially, GI planets are born as fluffy (gas density $\rho \sim 10^{-13}$ g/cm^3) and cold (T$\sim$ 100 K) molecular gas fragments. In order to become dense Jupiter-like giant planets, they must first contract to $T \gtrsim 2500$ K at which point a rapid dynamical collapse occurs (e.g., Bodenheimer 1974). Tantalisingly, if the planets migrate inward more rapidly than they contract, then they may be tidally disrupted. The disruption leaves behind a rocky/icy core if grains inside the planet managed to grow and sediment down into a core rapidly enough (McCrea & Williams 1965; Boley et al. 2010). This scheme, named "Tidal Downsizing" by Nayakshin (2010a), may *potentially* explain any mass planets at arbitrary separation from the host star within a single framework (Forgan & Rice 2013).

Here we focus on giant gas planets within the GI/TD framework specifically. While the rapid (migration time $t_{\rm mig} \sim 10^4$ years, see, e.g., Baruteau et al. 2011; Nayakshin 2010a) inward migration and tidal disruption process of gas fragments is crucial to TD as a way of accounting for terrestrial-like planets, this processes challenges the formation of the gas giants themselves (Zhu et al. 2012). Firstly, since radiative contraction time of even the Solar metallicity clouds is quite long ($\sim 10^6$ years, see, e.g., Bodenheimer et al. 1980; Vazan & Helled 2012), the disruption process appears to be too efficient (see §2.1), so it is hard to explain how *any* close-in giant planets survive. Secondly, radiative contraction of planets is slowed down at higher grain opacities (Helled & Bodenheimer 2011). Thus, tidal disruption in metal-rich environments should be even more efficient. This would seem to contradict the well known fact that giant planets are more abundant at higher metallicities (e.g., Fischer & Valenti 2005; Wang & Fischer 2013). If this is true then close-in giant planets must form via Core Accretion rather than GI (see, e.g., Boley 2009).

There may appear to exist a simple solution to the conundrum of too long a radiative cooling time for GI clumps: a strongly decreased grain opacity due to grain growth. Helled & Bodenheimer (2011) find that in models that include grain growth, opacity decrease cuts the planet contraction time scale to as short as $\sim 10^3$ years. We do not favour this solution for two reasons. Firstly, this would predict that protoplanetary discs of low metallicity stars would be ideal sites for gas giant planet formation. Instead, Fischer & Valenti (2005) shows that low metallicity stars

are the least likely to host a giant planet. Secondly, models of Helled & Bodenheimer (2011) do not include collisional fragmentation of dust grain aggregates which are found to occur at relatively modest velocities in laboratory experiments (e.g., Blum & Wurm 2008). Dullemond & Dominik (2005) consider grain growth and opacity in protoplanetary discs of T Tauri stars. They find that models that neglect grain growth deplete the small grain population by a factor of a million in a few thousand years (see their figure 3), reducing the dust opacity significantly. However, the spectra of T Tauri sources clearly require a copious presence of small dust grains even at ages of a few Million years. To explain this, Dullemond & Dominik (2005) argue that high speed dust aggregate fragmenting collision must be also taken into account. This then results in a quasi steady-state for dust distribution in which the smallest grain abundance is suppressed only mildly even after about a Million years of grain growth (see their Fig. 7). For these two (observationally backed up) reasons, we discount the possibility that grain opacity in GI fragments is much lower than the interstellar one, although we do explore some grain opacity reduction below.

The solution to the too-slow-cooling conundrum that is proposed here is based on another unexpected effect that grains have on GI clumps. Nayakshin et al. (2014) investigated the structure of the gas "atmosphere" around the massive solid core built within the TD gas fragments by grain settling. Similar to CA theory, it was found that there exists a critical core mass, $M_{\rm crit}$, beyond which the atmosphere may become self-gravitating and too massive to be in hydrostatic balance (Mizuno 1980; Stevenson 1982). Following CA arguments, the authors argued that the atmosphere collapse sets off a phase of a rapid gas accretion onto the dense core. This may initiate a hydrodynamical collapse (termed Core-Assisted Gas Capture instability; CAGS hereafter) of the whole gas fragment *before* a core-less fragment of same configuration would have collapsed, thus providing a second and an unexplored way for the formation of giant planets in the TD picture.

The original goal of this project was to follow up the work of Nayakshin et al. (2014) with a hydrodynamical rather than hydrostatic code, and to model the whole gas clump rather than only its centre. In addition, we included external large grain deposition onto the planet, the so-called "pebble accretion" (e.g., Johansen & Lacerda 2010; Ormel & Klahr 2010) of grains on massive bodies embedded in protoplanetary discs. In doing so we discovered that planets accreting grains can collapse more rapidly than those of fixed metallicity. It turned out that this effect has nothing to do with formation of the core directly, and instead originates in the fact that grain accretion on a planet in itself is a form of cooling. Pending detailed analysis below, this last statement can be understood qualitatively as follows.

Consider the total energy of the pre-collapse planet of mass $M_{\rm p}$ and radius $R_{\rm p}$, $E_{\rm tot} \sim -GM_{\rm p}^2/R_{\rm p}$. It evolves in time according to

$$\frac{dE_{\rm tot}}{dt} = -L_{\rm rad} - \frac{GM_{\rm p}\dot{M}_z}{R_{\rm p}} \ , \qquad (1)$$

where $L_{\rm rad}$ is the radiative luminosity of the planet, and the last term on the right is the change in the gravitational potential energy of the planet, $E_{\rm grav}$, due to grain accretion on it at the rate $\dot{M}_z$. In the constant metallicity case (no pebble accretion) that was so far studied in literature (Helled & Bodenheimer 2011), the second term on the right is absent, so that radiation is the only way for the planet to loose excess energy and contract towards H_2 collapse. Increasing metallicity of the planet increases dust opacity and decreases $L_{\rm rad}$, hence slowing down its contraction. However, if $\dot{M}_z > 0$, then the planet "cools" due to addition of metals, since $E_{\rm tot}$ becomes more negative. Deposition of pebbles into a planet from outside may hence speed up rather than delay giant planet formation.

The goal of this paper is to study the contraction of pre-collapse giant planets due to grain accretion in detail. To not over-complicate this first study by having to also study GAGC, we turn off grain growth in the planet, with the result that grain sedimentation is negligible, and no core forms in the planet's centre. The more general case is to be studied in a near future paper. We use a 1D spherically symmetric radiation hydrodynamics code as well as analytic arguments to understand the planet's response to pebble deposition.

The paper is structured as follows. In §2, the cooling challenge of GI-born fragments is described, and the rate of pebble accretion from the surrounding protoplanetary disc is estimated. In §3 and in Appendix A, numerical methods employed here are presented. §4 compares the evolution of planets enriched by metals either at birth or by pebble accretion, and §5 outlines an analytical toy model that helps to understand why metal accretion accelerates planet contraction. The analytical model is compared with grain-dominated contraction of numerically integrated polytropic clouds with fixed specific heats ratios (γ), as well as a more realistic molecular planet in §6. The conditions under which pebble accretion dominates planet contraction are delineated in §7. A discussion is given in §8.

2 PRELIMINARIES

2.1 The cooling challenge

The properties of the first gas condensations in a self-gravitating disc should be similar (Nayakshin 2010b) to that of the "first cores" (Larson 1969) in star formation, see also Bodenheimer (1974); Bodenheimer et al. (1980). The central temperature of these may be as low as $\lesssim 100$ K, Hydrogen is molecular, and the mass of the fragment is of the order of a Jupiter mass to perhaps $10\,{\rm M_J}$ (Boley et al. 2010; Forgan & Rice 2011; Tsukamoto et al. 2014). If the fragments cool sufficiently rapidly, reaching the central temperature of ~ 2500 K *before* they are tidally disrupted, then dissociation of molecular hydrogen occurs. Since post-collapse fragments are $\sim 3-5$ orders of magnitude denser than pre-collapse ones, post-collapse fragments are much more likely to survive as giant planets. H_2 collapse is hence a necessary step to formation of a gas giant planet.

However, radiative cooling times of isolated Jupiter-mass pre-collapse fragments are $t_{\rm rad} \sim 10^6$ years (e.g., Bodenheimer et al. 1980), far longer than the disc migration times, $t_{\rm mig} \sim 10^4$ years (e.g., Baruteau et al. 2011; Nayakshin 2010a). Figure 1 shows the radiative cooling time of the pre-collapse planets, defined as

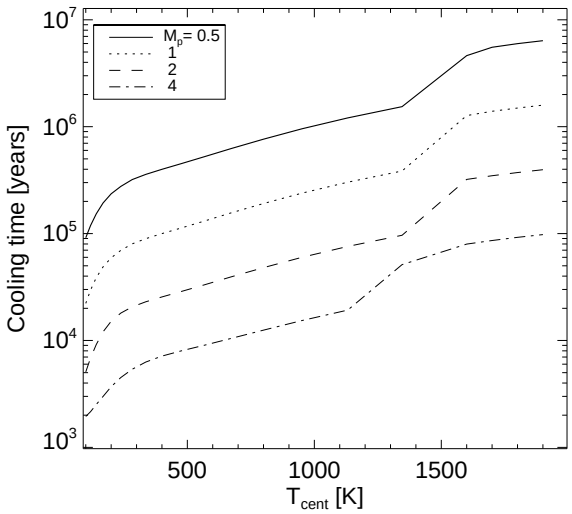

Figure 1. Radiative cooling times of pre-collapse planets of four different masses composed of a Solar mix of H/He and metals, as labelled on the figure, versus the central temperature of the planet, T_c. Note that low mass planets are the least capable of contracting rapidly, and that the slowest evolution always occurs at $T_c \gtrsim 1000$ K. Interstellar dust opacity is assumed for this figure.

$$t_{\rm rad} = -\frac{E_{\rm tot}}{2L} \ , \qquad (2)$$

where $E_{\rm tot}$ is the total energy of the fragment, and L is the luminosity of the planet. The factor 2 in the denominator is introduced empirically to better match the numerical calculations of planet contraction (all the way to H_2 dissociation) reported below.

In accord with previous results (Bodenheimer et al. 1980; Helled & Bodenheimer 2011), figure 1 shows that more massive planets cool more rapidly. Also note that, for all planetary masses, the initial cooling phase at T_c of a few hundred K is much more rapid when the one at $T_c \gtrsim 1000$ K. This is because the modulus of the total energy of the planet, $|E_{\rm tot}|$, increases, whereas the luminosity $L(T_c)$ usually drops with increasing T_c since the planet contracts and opacity in the atmosphere rises. This implies that the cooling "bottle neck" for planets of any mass is always at $T_c \gtrsim 1000$ K, that is, the planets are expected to spend more time contracting from $T_c \sim 1000$ K to H_2 dissociation ($T_c \sim 2200$ K or so, for most of our runs below) than they spend contracting from their initial state towards $T_c \sim 1000$ K.

Based on figure 1, the expected outcome of GI fragment contraction, while it also migrates inward rapidly, is that the fragment is tidally disrupted before it collapses (Boley et al. 2010; Nayakshin 2010a). For example, for $M_{\rm p} = 2\,{\rm M_J}$, it takes more than 10^5 years for this collapse to take place. Furthermore, calculations by Cameron et al. (1982); Vazan & Helled (2012) show that irradiation from the parent star and the surrounding disc slows the contraction of the fragments further, and may in fact even reverse the heat flow from the planet. In this case the planet puffs up rather than contracts with time. In the presence of tidal shear from the parent star, this is clearly a receipt for destruction rather than formation of a giant planet-to-be.

2.2 The role of metals

Giant planets are observed to be over-abundant in metals by a factor of a few to ten in the Solar System and beyond (Miller & Fortney 2011). Helled & Bodenheimer (2011) have shown that contraction of pre-collapse giant planets is slowed down further at high metallicites if dust opacity is proportional to the metallicity of the gas.

In the context of GI/TD models, we see two principal modes of metal enrichment of pre-collapse fragments. Firstly, fragments can be enriched by solids at birth by efficient aerodynamic capturing of grains into spiral arms of the gravitationally unstable disc before it collapses onto fragments (e.g., Boley et al. 2011). In this model, therefore, pre-collapse planets are born more metal rich than the surrounding disc. For simplicity, we then assume that the metallicity of such planets remain constant with time. Secondly, metals can be gained by accretion from the disc, as we explain now.

2.3 Accretion of metals from the disc

Johansen & Lacerda (2010) and Ormel & Klahr (2010) pointed out that "pebbles", that is small solid bodies of $\sim$ 10 cm-size can accrete efficiently on planetesimals and rocky protoplanets embedded in a disc. This can potentially speed up assembly of massive solid cores at tens of AU distances from the host star, where core accretion via planetesimal capture is inefficient, and solve the problem of too long core assembly time scale of CA theory (e.g., Helled & Bodenheimer 2014) for planets such as Neptune and Uranus.

In this picture, the accretor follows a Keplerian circular orbit of radius a_p around the star of mass M_*, whereas the gas in the disc moves at a velocity slightly smaller than the local Keplerian, and there is also the local Keplerian shear, so that there is always gas streaming past the accretor. The gas itself does not accrete onto the accretor since the gravity of the latter is insufficient to overcome the pressure gradient force of the gas. The small grains, on the other hand, are not supported against accretion onto the protoplanet by a pressure gradient.

A similar situation may hold around a much more massive molecular gas fragment. Nayakshin & Cha (2013) show that radiative pre-heating of the surrounding disc material by the radiation from a young embedded protoplanet is important in deterring gas accretion onto relatively low mass proto-planets, $M_{\rm p} \lesssim 6\,{\rm M_J}$. Such planets are found to build a hydrostatic-like atmosphere around themselves. The gas pressure gradient around them is large enough to prevent accretion of gas from the disc. Fragments with initial masses $M_{\rm p} \lesssim 6\,{\rm M_J}$ are found to migrate inward rapidly at more or less constant fragment mass until they are tidally challenged and eventually destroyed at $R \sim 20 - 30$ AU. More massive protoplanets instead accrete gas rapidly, becoming proto brown dwarfs and stalling at about their initial locations ($R \sim 80$ AU). These results imply that, as far as planet formation is concerned, we need to limit our attention to relatively low mass gas fragments of a few Jupiter masses as more massive fragments may form low mass stars, and eventually turn the system into a stellar binary, a situation that is well outside the scope of this paper.

Lambrechts & Johansen (2012) recently presented ana-

lytical estimates and numerical simulations of pebble accretion on large planetesimals and solid cores. We rescale their results to the case of a pre-collapse giant planet embedded in a protoplanetary disc. Due to the substantial mass of the planet (compared to planetesimals or solid cores), the accretion of **pebbles** on it is always in the "Hill's regime", when **pebbles** are accreted from the whole of the Hill's radius, $R_{\rm H} = a_p(M_{\rm p}/3M_*)^{1/3}$, where a_p is the planet-star separation, and M_* is the mass of the host star. The maximum rate, $\dot{M}_{\rm z}$, at which the grain particles can be accreted by the planet in the this regime is (see eq. 38 in Lambrechts & Johansen 2012)

$$\max \dot{M}_z = \dot{M}_{\rm H} \approx 2R_{\rm H}\Sigma_{\rm dust}v_{\rm H} \ , \quad (3)$$

where $\Sigma_{\rm dust}$ is the **pebbles** surface density in the protoplanetary disc, Hill's velocity is $v_{\rm H} = \Omega_p R_{\rm H}$, and Ω_p is the Keplerian angular speed at the location of the planet. In reality only grains intermediately strongly coupled to the gas, such that dimensionless stopping time, $\tau_f \equiv t_f\Omega_p$, $0.1 \lesssim \tau_f \lesssim 1$ are accreted as efficiently as equation 3 suggests. **The physical size of the particles in the strongly coupled regime, that is "pebbles" in our definition, depends on the protostellar disc properties and the radial distance from the star, R. For the Minimum Mass Solar Nebula disc, Lambrechts & Johansen (2012) show that particles of size $a \sim$ a few cm $\times R_1^{-3/2}$ are in the pebble regime, where $R_1 = R/(10$ AU$)$. Thus, at the outer disc regions, $R \sim 100$ AU, pebble regime grains are actually about 1 mm or so.**

Let us define the planet metallicity doubling time scale t_z as

$$\frac{1}{t_{\rm z}} \equiv \frac{\dot{M}_{\rm z}}{M_{\rm z}(0)} \ , \quad (4)$$

where $M_z(0) \equiv z_0 M_{\rm p}$ is the initial mass of metals in the planet. Let the fraction of mass in the **pebble regime**, that is, in the maximum efficiency accretion regime (compared to the total mass in grains in the disc at radius a_p) be $f_{\rm max} < 1$. Further, $\Sigma_{\rm dust} = z_0\Sigma \sim z_0 M_{\rm disc}/(\pi a_p^2)$, where Σ is the total (dust plus gas) surface density of the disc, $M_{\rm disc}$ is the disc mass at radius a_p, and we assumed that the disc metallicity is equal to the initial metallicity of the planet, z_0. The end result is,

$$t_{\rm z} \approx \frac{1}{2f_{\rm max}} \frac{M_{\rm p}^{1/3} M_*^{2/3}}{M_{\rm disc}} \frac{2\pi}{\Omega_p} \ . \quad (5)$$

Now, in the early massive protoplanetary disc stage that is of interest here, the disc can be as massive as $0.1M_*$ or more. Picking this value for $M_{\rm disc}$ and $M_{\rm p} = 1\,{\rm M_J}$, we then have

$$t_{\rm z} \sim 10^3 \text{ years } \frac{1}{2f_{\rm max}} \Big(\frac{a_p}{100AU}\Big)^{3/2} \ . \quad (6)$$

This shows that if the population of large grains is significant, e.g., $f_{\rm max} \gtrsim 0.1$, then the time scale to double the initial metal content of the gas fragment is comparable or shorter than the typical migration time, $t_{\rm mig} \sim 10^4$ years (Nayakshin 2010a). Tidal Downsizing planets may then be non-trivially over-abundant in metals by the time they migrate into the inner few AU of the protoplanetary disc region.

Clearly, $\dot{M}_{\rm z}$ and $t_{\rm z}$ are functions of the disc properties, of the planet's location within the disc. Further, the disc itself may be influenced by the interaction with the planet. For now we explore the case of a fixed $t_{\rm z}$, in which the planet is loaded by pebbles (metals) from outside at a constant rate as given by equation 4. The value of $t_{\rm z}$ is varied in a broad range to study the parameter space.

3 NUMERICAL METHODS

The code used here is a spherically symmetric Lagrangian hydrodynamics code first described in Nayakshin (2010b), expanded and updated since then as detailed in Nayakshin (2011a,b, 2014). Here we actually simplify the dust-gas interactions module of the code to expose the metal-loading effect most clearly. The simplified set of equations permits a comparison with analytical solutions, which serves as a check of both the code and our physical intuition. In the papers cited just above, the focus was on formation of dense metal cores inside the fragment, and hence the relative dynamics of gas and pebbles within the fragment was important and modelled by two-fluid equations with aerodynamical gas force coupling the two species. In this paper, we turn off grain growth and vaporisation physics, assuming that grains are always "small", setting $a = 1\mu$m. In practice this means that there is no relative motion of gas and grains and hence our equations reduce to the standard one-fluid gas-dynamical equations. Physically, this limit corresponds to the case when grains deposited into the outer reaches of the planet either do not grow sufficiently rapidly or get vaporised quickly if the fragment is too hot (e.g., water ice is vaporised already at $T \sim 150$ K). The grains can however be mixed in with the gas throughout the cloud quickly by convection and turbulence (e.g., Helled et al. 2008; Nayakshin 2011b; Helled & Bodenheimer 2011), so that the metallicity of the planet (related to the grain to gas mass ratio) is set to be uniform inside the planet at all times. The more complicated situation, where a relative gas-grain motion does occur, is of course of a significant interest as well, but, due to a considerably expanded parameter space in that case (e.g., has the core formed or not, and what is the chemical composition of that core?) it is to be presented in the near future elsewhere. We emphasise that the "metal loading" effect presented here exists when the grains are allowed to sediment as well; it is however not possible to study that analytically since grains are redistributed within the planet in a complicated way.

Following Helled & Bodenheimer (2011), we make a reasonable assumption that dust opacity in the fragment is directly proportional to the metallicity of the gas, z. The opacity $\kappa(\rho, T)$ is then given by

$$\kappa(\rho, T) = f_{\rm op}\kappa_0(\rho, T)\frac{z}{z_\odot} \ , \quad (7)$$

where $\kappa_0(\rho, T)$ are the interstellar gas plus dust opacities from Zhu et al. (2009) which assume Solar metallicity, $z_\odot$, and $f_{\rm op} = {\rm const} \leqslant 1$ is a positive constant, set to 0.1 everywhere in this paper, to account for possible opacity reduction due to grain growth. The main conclusions of our paper are unchanged irrespectively of the value of $f_{\rm op}$, except that the parameter space where metal loading dominates as a cooling process of course does depend on $f_{\rm op}$, as described below in §7.

The full set of equations being solved for numerical experiments in this paper is presented in the Appendix. The initial conditions are polytropic spheres of a given central temperature $T_{\rm c}$, metallicity (usually Solar metallicity), and total mass $M_{\rm p}$.

4 THE METAL LOADING "PARADOX"

Figure 2 shows contraction calculations for a planet of $M_{\rm p} = 4\,{\rm M_J}$ masses, with grain opacity reduced by a factor of 10, performed under two different assumptions about the planet's grain content. The left hand panels show the cases of constant planet metallicity (enrichment at birth model), where $z = 0.5, 1$ and 2 times the Solar metallicity. The right hand panels show the same calculation but for the planets all starting with the Solar grain abundance at $t = 0$ and then metal-loaded by pebble deposition at five different (constant) rates as labelled on the figure. In particular, the curves are computed for metal loading times ranging from $t_z = 250$ years to $t_z = 4000$ years, in steps of a factor of 2. Note that the shortest t_z values are unlikely to be reached even in the inner disc regions (unless radial drift of pebbles, see Lambrechts & Johansen 2014, significantly increases the local pebble abundance). However, such cases expose the metal loading effects clearly. In a follow up paper (Nayakshin 2014, submitted), the pebble accretion rate is calculated self-consistently from the surrounding disc properties, which is modelled in some detail similarly to Nayakshin & Lodato (2012).

The constant metallicity cases, panels (a) and (b), are in a qualitative agreement with results of Helled & Bodenheimer (2010). The time taken by the planet to contract to the point of collapse increases with increasing z, somewhat less rapidly than a linear proportion.

Panels (c) and (d) show a completely different evolution, however. The more rapidly the metals are added to the planet, the more rapidly it contracts and eventually collapses via H_2 dissociation. In the most rapid metal-loading case, $t_z = 250$ years, the collapse time scale is shortened by a factor of almost four compared with the Solar metallicity case. For this particular case, the metallicity at collapse is $z \approx 0.12$, eight times larger than the starting value, $z_0 = 0.015$. Based on the left hand side panels, one would expect that collapse time scale for such a high metallicity fragment would be a factor of ~ 5 longer than the solar metallicity case, not shorter. There is thus over an order of magnitude difference in the collapse time scale for this particular case between the enrichment at birth and a gradual metal deposition models.

Figure 3 shows another numerical experiment that helps to shed more light on the situation. The planets here are started exactly as the ones presented in figures 2c and 2d, with the same choices for the metal doubling time, but grain accretion is termined when the central temperature reaches $T_{\rm c} = 700$ K. The exact numerical value of the termination temperature is not important. Figure 3 shows that once grain accretion stops, contraction of the cloud continues *at a slower* rate than that for a non-metal-polluted planet, i.e., one recovers the main result of the fixed metallicity cases shown in figure 2a and 2b. For example, for the case of the most rapid metal loading, $t_z = 250$ years, the fragment collapsed at less than 2,000 years in figure 2(a), but collapses only at $t \approx 9,000$ years when grain accretion is discontinued.

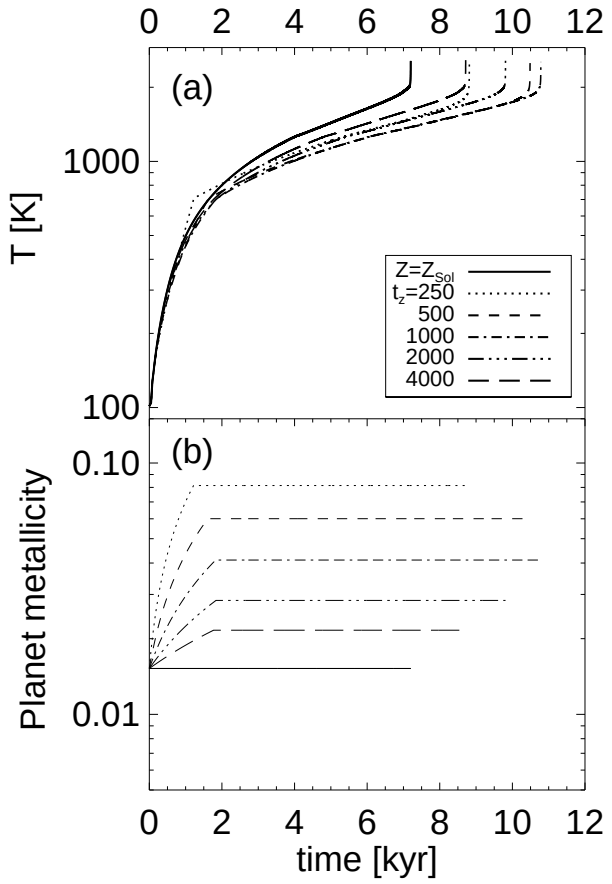

Figure 3. Same as the right hand side panels of figure 2 but grain accretion is (arbitrarily) turned off once the central temperature of 700 K is reached. Note that the faster the metals are loaded, the faster the fragments contract, but once grain accretion stops the situation reverses; the more metals are in the planet, the slower it contracts.

These results indicate that pebble deposition into a pre-collapse planet produces two opposing effects, one delaying contraction of the planet, and the other speeding it up. The former effect is due to the increase in the dust opacity which slows down radiative contraction of the fragment. In our opacity model, this effect depends on the instantaneous amount of dust in the planet, that is, its metallicity. The latter effect however depends not on the amount of dust in the planet but on the rate of grain deposition into the planet, as hinted in the Introduction.

5 A TOY MODEL

To understand how grain accretion can accelerate collapse of a planet we turn to a simple analytical model in which the planet is modelled as a polytropic sphere of adiabatic index $\gamma = 1 + 1/n$. The equation of state (EOS) of the gas in the sphere is

$$P = K\rho^{\gamma}\ , \qquad (8)$$

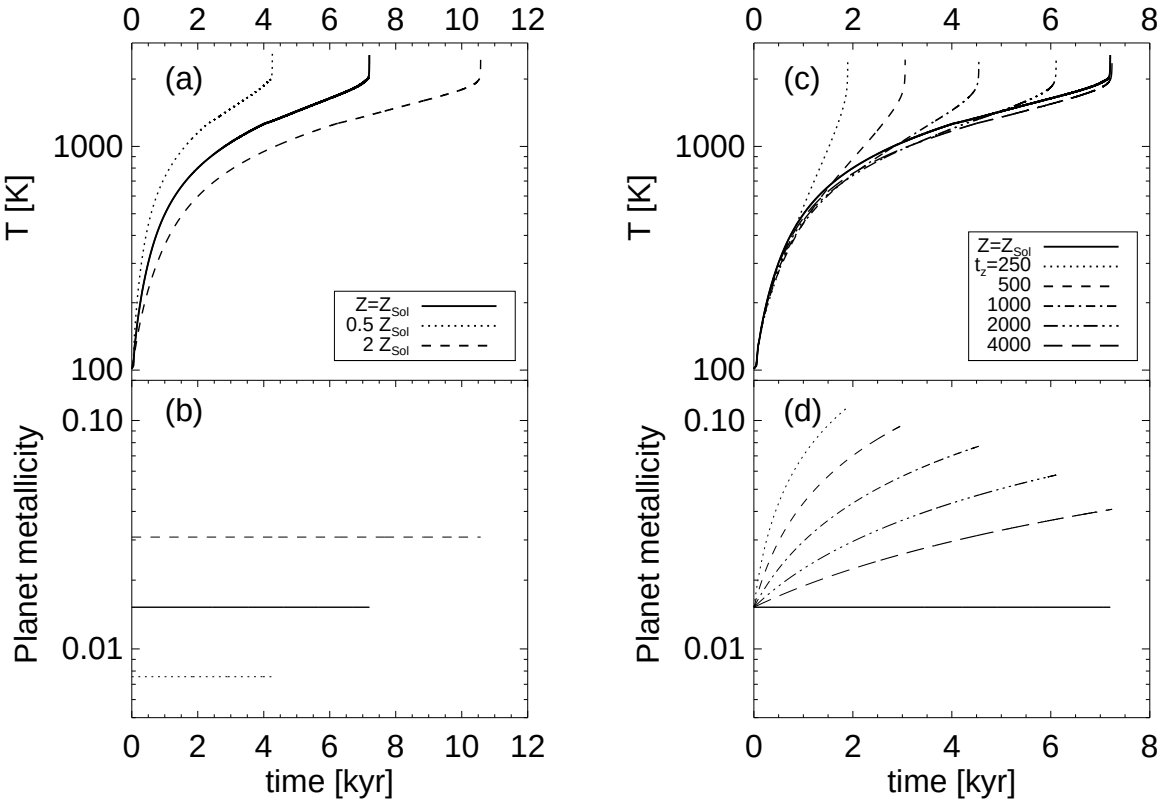

Figure 2. Top left panel (a): evolution of the central temperature versus time for constant metallicity planets of $4\,\mathrm{M_J}$ masses. The bottom left panel (b) shows the (constant in time) metallicity, z, of the planets. Right panels (c) and (d): same but for planets loaded by grains at constant rates parameterised by the metallicity doubling time t_z. Note that the faster the metals are added to the planet, the quicker it collapses.

where P and ρ and the total (gas plus metals) pressure and density, respectively, and K is a constant throughout all of the planet. Constancy of K is assumed to be maintained by convection that is known to be the main energy transfer mechanism within H_2 dominated planets (e.g., Helled & Schubert 2008).

The theory is only approximate, since there is no single value of γ that could describe a planet dominated by molecular hydrogen exactly. For gas dominated by molecular hydrogen, γ varies from $\gamma = 5/3$ at $T \lesssim 100$ K to $\gamma = 7/5$ in a relatively broad temperature range, $200 \lesssim T \lesssim 1000$ K, and finally drops to $\gamma \approx 1.1-1.2$ at $T \gtrsim 1500$ K (see figure 5a below, and Boley et al. 2007). An H_2 dominated gas fragment spans a range of temperatures, from the maximum at the centre, T_c, to the minimum at the atmosphere of the planet, $T_{\rm eff}$, which may be as low as tens of K (Vazan & Helled 2012), so γ varies within the planet significantly. However, qualitatively, H_2 dominated gas fragments behave as polytropes with γ varying from 5/3 at low T_c to $\gamma < 4/3$ at $T_c \gtrsim 2000$ K.

The total energy of a polytrope of mass M_p and radius R_p is (e.g., Chandrasekhar 1957)

$$E_{\rm tot} = -\frac{3-n}{5-n}\frac{GM_p^2}{R_p} \equiv -\frac{3\gamma-4}{5\gamma-6}\frac{GM_p^2}{R_p}\ , \qquad (9)$$

For $\gamma < 4/3$, the total energy of the planet changes sign, which marks the dynamical instability to gravitational collapse for gas with $\gamma < 4/3$. In the context of molecular hydrogen dominated fragments, the instability leads to H_2 molecules dissociation and the gravitational collapse of the planet.

Consider now an instantaneous addition of grains of mass $\delta M_z \ll M_z \ll M_p$ throughout the planet, where M_z is the current mass of metals in the planet, so that grain mass added within radius R is $\delta M = (M/M_p)\delta M_z$, where M is planet's mass interior to $R < R_p$. If grains are not vaporised, then the thermal energy of the gas/grain mixture does not vary appreciably due to this addition (kinetic energy in Brownian motions of grains is negligible since the weight of a grain is much larger than that of H_2 molecule). However, there is a change in the gravitational potential energy of the planet,

$$\delta E_{\rm grav} = -\int_0^{M_p}\left(G\frac{M+\delta M}{R}\left[dM + d\delta M\right] - \frac{GM}{R}dM\right)\ . (10)$$

Assuming that R does not vary during this instantaneous mass variation, and since $\delta M/M = \delta M_z/M_p = \text{const}$,

$$\delta E_{\rm grav} = 2\frac{\delta M_z}{M_p}E_{\rm grav}\ , \qquad (11)$$

where $E_{\rm grav} = -\int(GM/R)dM = -(3/(5-n))GM_p^2/R_p$. Due to energy conservation, $\delta E_{\rm tot} = \delta E_{\rm grav}$, and hence total energy of the planet evolves according to

$$-\frac{3-n}{5-n}\frac{d}{dt}\frac{GM_{\rm p}^2}{R_{\rm p}} = -\frac{6}{5-n}\frac{GM_{\rm p}^2}{R_{\rm p}}\frac{\dot{M}_z}{M_{\rm p}} \ . \quad (12)$$

Now, since grain accretion is the only mass gain term for the planet, $\dot{M}_p = \dot{M}_z$, and so equation 12 integrates to

$$\ln\frac{GM_{\rm p}^2}{R_{\rm p}} = \frac{6}{3-n}\ln M_{\rm p} + {\rm const} \ . \quad (13)$$

It is apparent that as $M_{\rm p}$ increases, $|E_{\rm tot}|$ increases as well (and rapidly if $n \to 3$). If $M_{\rm p}^0$and $R_{\rm p}^0$ are the initial planet mass and radius before grain accretion sets in, then the constant in the above equation can be eliminated, resulting in

$$\frac{GM_{\rm p}^2}{R_{\rm p}} = \left(\frac{GM_{\rm p}^2}{R_{\rm p}}\right)_0 \left[\frac{M_{\rm p}}{M_{\rm p}^0}\right]^{\frac{6}{(3-n)}} \quad (14)$$

The planet's mass is the sum of the mass of the gas and that of metals, $M_{\rm p} = (1-z)M_{\rm p} + zM_{\rm p}$, and $M_{\rm gas} = M_{\rm p}(1-z) = {\rm const}$. Thus, $M_{\rm p}/M_{\rm p}^0 = (1-z_0)/(1-z)$, where z_0 is the initial metallicity of the planet. Equation 14 can be now rewritten in terms of changing metallicity of the planet rather than its total mass.

Provided that the mean molecular weight of the gas, μ, is known, one can find the central temperature of the polytrope,

$$T_{\rm c} = A_n\frac{GM_{\rm p}\mu}{k_{\rm b}R_{\rm p}} \quad (15)$$

where $A_n = -[(n+1)\xi_1\theta_n']^{-1} \sim 1$ is a function of n but not $M_{\rm p}$ or $R_{\rm p}$. For $n = 5/2$, $A_n \approx 0.7$. Since we neglect metal's contribution to pressure and internal energy of the mix and assume a homogeneous spreading of metals inside the planet, $\mu \approx \mu_0 M_{\rm p}/M_{\rm g} = \mu_0/(1-z)$, where μ_0 is the mean molecular weight of H_2/He mixture. From equation 15, $T_{\rm c} \propto GM_{\rm p}^2/R_{\rm p}$, leading to

$$T_{\rm c} = T_0\left(\frac{M_{\rm p}}{M_{\rm p0}}\right)^{\frac{6}{3-n}} = T_0\left[\frac{1-z_0}{1-z}\right]^{\frac{6}{3-n}} \ . \quad (16)$$

This equation describes how temperature of the planet increases as its metallicity increases. In the limit $z_0 < z \ll 1$ it can be further simplified by writing $(1-z_0)/(1-z) \approx 1+(z-z_0)$, and using the identity $(1+x)^b \approx \exp(bx)$ valid for $x \ll 1$:

$$T_{\rm c} = T_0\exp\left[\frac{6\Delta z}{3-n}\right] \ , \quad (17)$$

where $\Delta z = z - z_0$. This shows that if $6/(3-n) \gg 1$ then the planet is very sensitive to addition of grains.

In particular, for di-atomic molecules, $\gamma = 7/5$, or $n = 5/2$, which yields

$$T_{\rm c} = T_0\exp\left[12\Delta z\right] = T_0\exp\left[0.18\frac{\Delta z}{z_\odot}\right] \ , \quad (18)$$

where $z_\odot = 0.015$, the Solar metallicity. This suggests that over-abundance of metals by a factor of $5-10$ in a gas fragment dominated by molecular hydrogen may significantly increase $T_{\rm c}$, taking the planet closer to the desired $T_{\rm c} \gtrsim 2000$ K point at which it can collapse to much higher densities.

Figure 4 show a comparison of the analytical theory (equation 16) with numerical integrations of the metal loading effect performed with our code, except that the H/He mix EOS was replaced by the polytropic gas equation with a fixed γ. Five values of γ are considered, as labelled on the figure. The metal loading time is $t_z = 300$ years for all of the curves. The black curves in top panel, fig. 4a, are numerical integrations, whereas red lines are equation 16. Figure 4b shows the metallicity evolution of the planets, which is identical, all given by same value of $t_z = 300$ years. The agreement between the theory and numerical simulations is acceptable to us. The curves show, just as equation 16 does, that the smaller the value of γ, the stronger the planet reacts to addition of grains. This is because $n = 1/(\gamma-1)$ edges closer to the unstable value, $n = 3$, as γ approaches 4/3 from above, and even a small amount of metals can cause a significant contraction of the planet.

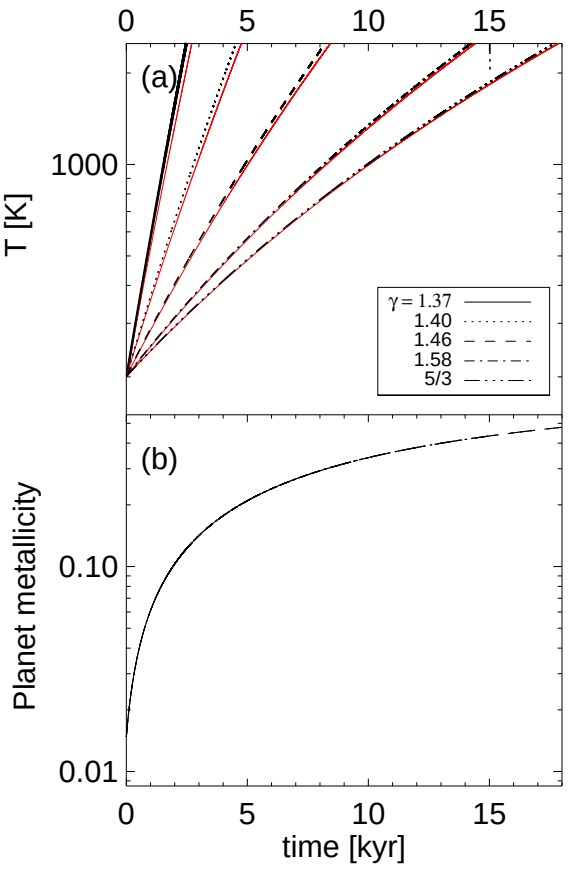

Figure 4. Evolution of polytropic gas fragments for five different values of γ, as labelled in the figure, when loaded with grains homogeneously throughout the cloud. The solid red lines are predictions of the analytical model (equation 16), whereas black curves are the results of the numerical integration.

The same result (equation 16) can be also obtained from a polytropic sphere relation between planet's radius, mass, and the "constant" K, if the latter is allowed to vary as z changes. Namely, $K = P/\rho^{1+1/n} = K_0[(1-z)/(1-z_0)]^{1+1/n}$ in this case, where K_0 is the polytropic constant at $z = z_0$. Since K is related to entropy per unit mass of the planet, this provides another interpretation of the metal loading effect: adding metals decreases entropy of the cloud, just as radiative cooling does, so metal accretion is effectively a cooling mechanism.

6 REAL H_2-DOMINATED POLYTROPES

Having explored idealised polytropic models with a fixed value of γ (or n), we turn to more realistic cases of H/He-dominated pre-collapse planets. Figure 5a shows adiabatic index γ versus gas temperature for a Solar composition H/He plus metals mix for the ideal EOS used in this paper calculated for a fixed gas density of $\rho = 10^{-7}$ g/cm^3. As expected, $\gamma = 5/3$ at $T \lesssim 100$ K when rotational and vibrational degrees of freedom of molecular hydrogen are not yet excited; then at higher T, γ drops to $\approx 7/5$ appropriate for diatomic gas. This persists until $T \sim 1500$ K when H_2 dissociation becomes energetically possible. Due to H_2 dissociation at temperatures around 2000 K, γ plunges to about 1.1.

Clearly, each pre-collapse planet configuration spans a range of densities and temperatures, from the maximum in the centre to the minimum in the atmosphere. To relate to the analytical theory derived in §5, we define effective γ and n for a planet by computing the gravitational potential energy of that planet and then comparing it with that of a polytropic planet of the same mass and radius, e.g.,

$$E_{\rm grav} = -\frac{3}{5-n}\frac{GM_{\rm p}^2}{R_{\rm p}} \ , \tag{19}$$

where $n = 1/(\gamma - 1)$. The values of the $\gamma_{\rm eff}$ versus planet's central temperature are plotted in figure 5a for two planetary masses, $M_{\rm p} = 1\,{\rm M_J}$ and $M_{\rm p} = 4\,{\rm M_J}$. These are very similar all the way to $T_{\rm c} \approx 2000$ K. As can be expected, $\gamma_{\rm eff}$ for a planet bears a strong resemblance to the $\gamma(T)$ function (the solid curve), except smoothed out somewhat due to the presence of a range of temperatures inside a planet, and also shifted to higher temperatures since $T_{\rm c}$ represents the maximum temperature in a given planet, whereas $\gamma_{\rm eff}$ is probably related more closely to a mean temperature in the planet.

Now, the analytical theory developed in §5 predicts how the central temperature of a polytropic planet varies with its metallicity when grains are added to the planet, e.g., $T_{\rm c} \propto (1-z)^{-\sigma_{\rm z}}$ (equation 16), where we defined "metallicity exponent"

$$\sigma_{\rm z} = -\frac{d\ln T_{\rm c}}{d\ln(1-z)} = \frac{6}{3-n} \ . \tag{20}$$

The dependence of σ_z on central temperature is plotted in figure 5b for the two planetary masses, and also for the solid curve from figure 5a (corresponding to fixed gas density of $\rho = 10^{-7}$ g/cm^3).

The dash-dotted curve passing through red triangles in the panel shows $-[d\ln T_{\rm c}/d\ln(1-z)]$ actually measured in simulations of planets of mass $M_{\rm p} = 4\,{\rm M_J}$ loaded with metals. These (short) runs are started with the planets initialised as polytropic spheres of Solar metal abundance following the ideal EOS with $T_{\rm c}$ shown on the horizontal axis. The metals are added to the planets in the same way as described in §4, with $t_z = 500$ years (the choice of t_z is unimportant for this plot). We then measure $\sigma_{\rm z}$ when z varies by a small increment. To make sure that radiative cooling of the planet, which also drives evolution of $T_{\rm c}$ in realistic planets, does not corrupt our measurement of $\sigma_{\rm z}$, we set the opacity multiplier to a very large number (10^{10}) to turn off radiative cooling of the planet for figure 5.

The dash-dotted curve (measured $\sigma_{\rm z}$) should be compared with the dashed one (predicted). These two are relatively close but do not coincide exactly, which probably reflects the fact that our definition of $\gamma_{\rm eff}$ in equation 19 is somewhat arbitrary, and is only one possible way to define an effective γ for a planet. Using the total energy of the planet to define γ, for example, gives slightly different values for $\gamma_{\rm eff}$. Nevertheless, the agreement appears reasonable and hence the analytical theory has some utility in explaining contraction of metal-loaded pre-collapse planets.

We also define the central temperature doubling metallicity, $z_{\rm d}$, as metallicity at which $T_{\rm c}$ is twice its initial value, T_0. Given the definition of $\sigma_{\rm z}$ and equation 16,

$$z_{\rm d} = 1 - (1 - z_0)\ 2^{-1/\sigma_{\rm z}} \tag{21}$$

where z_0 is the initial planet's metallicity. The doubling metallicity in units of Solar metallicity, and assuming $z_0 = z_\odot$, is plotted in figure 5c for the same models as in the two panels above it. We can see that metal over-abundance of a factor of a few to ten in Solar metallicity units is required to cause the planet to shrink by a factor of two in radius (planet's radius is nearly exactly inversely proportional to $T_{\rm c}$). The required metal over-abundance is smaller at higher temperatures because the planet is closer to the unstable value of $\gamma = 4/3$ at higher $T_{\rm c}$.

7 GRAIN-DOMINATED PLANET COLLAPSE

Having studied the contraction rates of planets loaded by metals, we can now ask the question of when such a contraction is faster than that due to radiative cooling. This happens when the rate of central temperature increase due to radiative cooling rate is equal to the that due to metal loading. The latter can be found via

$$\frac{dT_{\rm c}}{dt} = T_{\rm c}\frac{d\ln T_{\rm c}}{d\ln(1-z)}\ \frac{d\ln(1-z)}{dt} \ . \tag{22}$$

Now, using equation 20 and definition $1-z = M_{\rm gas}/(M_{\rm gas} + M_{\rm z})$, where $M_{\rm gas}$ and $M_{\rm z}$ and the total mass of gas and metals in the planet, we write

$$\frac{d\ln(1-z)}{dt} = -\frac{1}{M_{\rm p}}\frac{dM_{\rm z}}{dt} = -\frac{M_{\rm z}(0)}{M_{\rm p}t_{\rm z}} \tag{23}$$

The condition of the two contraction rates being equal to each other reads

$$\frac{T_{\rm c}}{t_{\rm rad}} = T_{\rm c}\sigma_{\rm z}\ \frac{z_0}{t_{\rm z}} \tag{24}$$

where we set $z = z_0$. This defines the critical metal loading time scale, $t_{\rm crit}$, such that if metals are supplied to the planet on a time scale shorter than $t_{\rm crit}$ then the planet contracts mainly due to the increasing metal content rather than radiative cooling. According to equation 24, the critical time is

$$t_{\rm crit} = t_{\rm rad}\sigma_{\rm z}z_0 \ , \tag{25}$$

Figure 6 plots the critical metal loading time versus planet's central temperature for the same range of planetary masses as in figure 1. The curves showing $t_{\rm crit}$ are qualitatively similar to those showing $t_{\rm rad}$ for obvious reasons save for the absolute values, and the factor $\sigma_{\rm z}$ that is a function of $T_{\rm c}$.

This figure shows that loading the planet by metals at a typical $t_{\rm z}$ of a few thousand years, as estimated in §2.3, is not

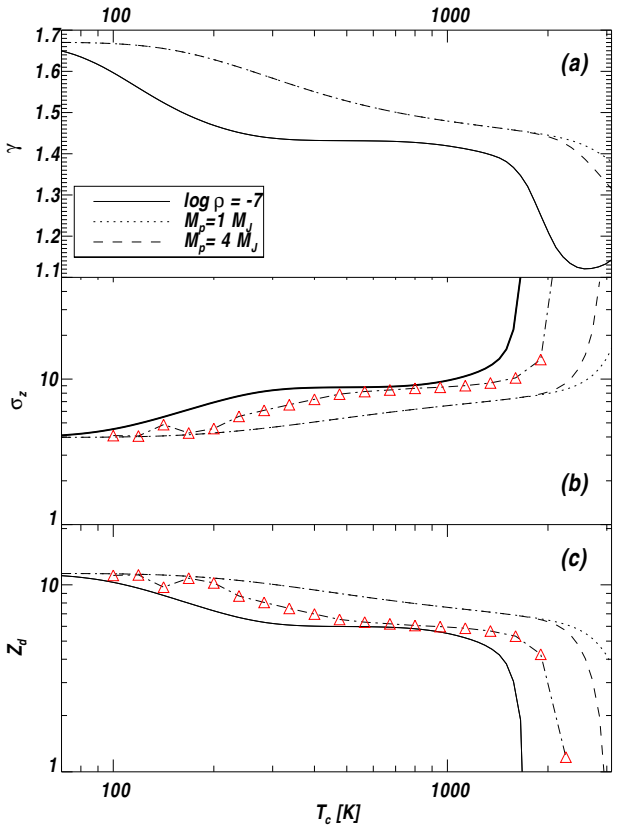

Figure 5. Panel (a): the ratio of specific heats, γ, for our Solar composition EOS at a fixed gas density, $\rho = 10^{-7}$ g/cm^3 (the solid curve), and the effective γ for two planetary masses as defined by equation 19. Middle panel (b): Metallicity exponent (equation 20) for the same cases as panel (a), plus one directly measured from a numerical experiment for $M_{\rm p} = 4\,{\rm M_J}$ (dot-dashed curve passing through triangles). The larger σ_z, the more rapidly planet contracts as metals are loaded into it. Panel (c): the central temperature doubling metallicity $z_{\rm d}$, defined by equation 21, for the same cases as in panel (b), and plotted in units of the Solar metallicity, $z_\odot$.

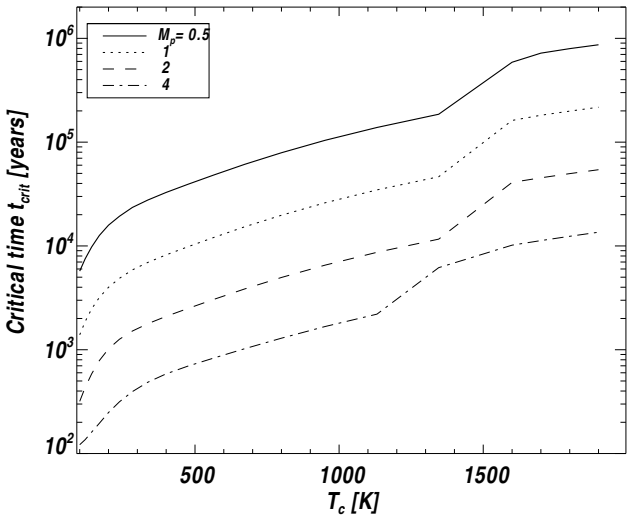

Figure 6. Critical metal-loading time versus planet's central temperature for four different planetary masses and interstellar grain opacities, as labelled in the box in the figure. Metals must be added to the planet rapidly, so that $t_z < t_{\rm crit}$, in order for the metal loading to dominate over radiative cooling as a contraction mechanism.

likely to affect relatively massive planets, $M_{\rm p} \gtrsim 2\,{\rm M_J}$, at the beginning of their evolution, but may affect them when they contract towards $T \gtrsim 1000$ K. This finding is consistent with the right panels of figure 2, in which the central temperature evolution of metal-loaded planets fed by metals at different rates was shown. The figure showed that early evolution of planets, when $T_{\rm c} \lesssim 500$ K, is indistinguishable for different $t_{\rm z}$, at least in a rather broad range of $t_{\rm z}$, from 250 years all the way to $t_{\rm z} = \infty$. This can now be understood in terms of the radiation-dominated phase of the planet's contraction: early on the planet contracts radiatively more rapidly than it does due to metal loading, even at the shortest $t_{\rm z}$ explored in the figure. At later times, however, depending on $t_{\rm z}$, the planets go off the fixed metallicity (solid curve in figure 2c) track and accelerate onto the metal-dominated part of their evolution.

On the other hand, figure 6 predicts that evolution of lower mass gas fragments may be much more sensitive to deposition of metals. For example, for $M_{\rm p} = 0.5\,{\rm M_J}$, even $t_{\rm z} = 10^4$ years is short enough to dominate fragment's contraction. One preliminary conclusion from this, which clearly needs to be explored more rigorously in a realistic evolving protoplanetary disc setting, is that lower mass giant planets formed by GI/TD may be more metal rich. Physically, it takes far longer for these planets to contract (because their radiative cooling times are much longer, see figure 1). For this reason, they are likely to have a lower central temperature for longer than their massive cousins. Based on the theory developed above and figure 5, their contraction due to metal loading is therefore slower, and hence they may be able to absorb more metals before they collapse.

While a full scale investigation of this prediction is outside the scope of our paper, figure 7 compares the evolution of two planets, $M_{\rm p} = 4\,{\rm M_J}$, which was already shown in figures 2c,d with the long dash curves, while the other planet has a lower mass, $M_{\rm p} = 1\,{\rm M_J}$. The solid lines in figures 7a,b show the evolution of the central temperature and metallicity, z, respectively, for $M_{\rm p} = 1\,{\rm M_J}$. The dashed curve in figure 7b show the ratio of the critical metal loading time scale to the actual value of $t_{\rm z}$ (4000 years for both runs). Except for the earliest times, that ratio is always greater than unity, suggesting that evolution of this planet is nearly always metal dominated. This planet collapses at $t = 0.12$ Myr almost entirely due to metal loading rather than radiation. By the time the planet collapses, its metallicity is very high, $z \approx 0.3$, e.g., some 20 times higher than $z_\odot$.

The evolution of the more massive planet is distinctly different. Since such planets are cooling much more rapidly (see fig. 1), metal loading is a relatively minor effect in this case, with $t_{\rm crit}/t_{\rm z} < 1$ everywhere (see figure 7d). The evolution of a massive planet is hence radiation-dominated. The critical loading time $t_{\rm crit}$ is calculated using equation 25, where the radiative time is found at each time step using the definition from equation 2, the metallicity exponent σ_z

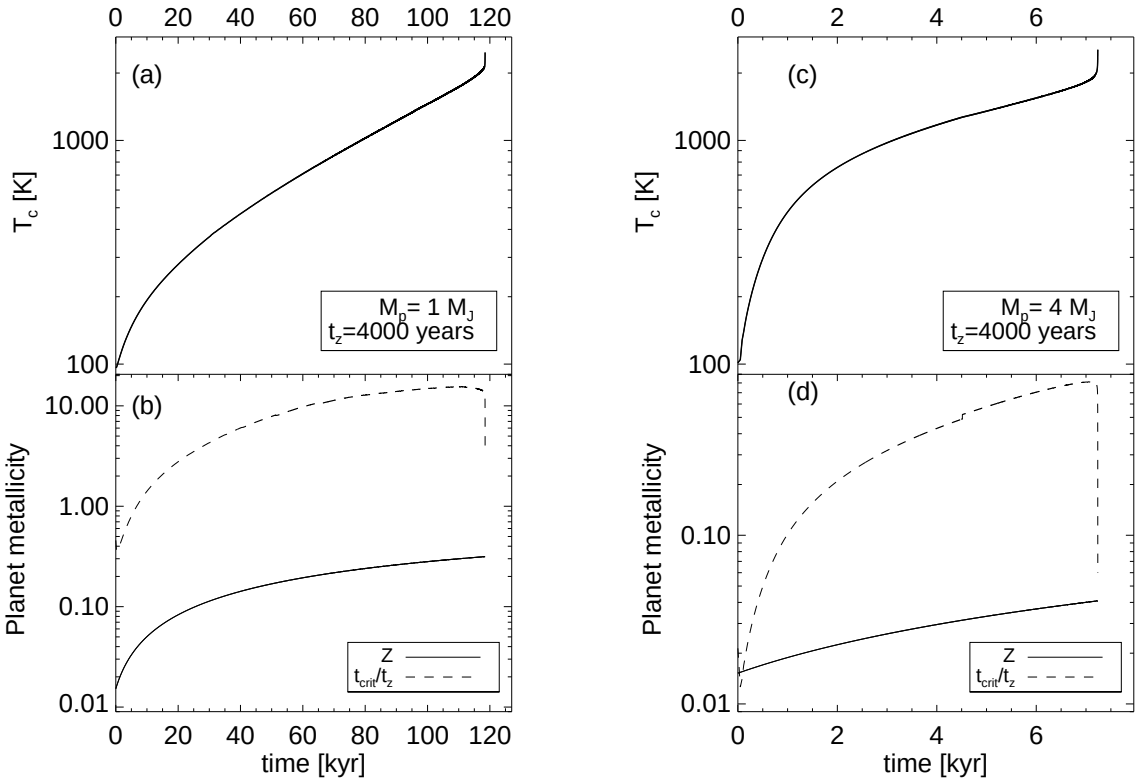

Figure 7. The central temperature (top panels, a and c) and metallicity (bottom panels, b and d) versus time for planets with mass $M_{\rm p} = 1\,{\rm M_J}$ and $M_{\rm p} = 4\,{\rm M_J}$ (left and right panels, respectively). The dashed curve in the bottom panels show the ratio of the critical metal loading time scale to the actual value of $t_{\rm z}$ (4000 years for both runs). The dashed curves show that the evolution of the $M_{\rm p} = 1\,{\rm M_J}$ is dominated by metal loading, whereas that of the $M_{\rm p} = 4\,{\rm M_J}$ is dominated by radiative cooling.

is computed using equation 20 and definition of n given by equation 19.

8 DISCUSSION

In this paper we have shown that accretion of pebbles from the surrounding protoplanetary disc is a surprisingly efficient way for pre-collapse H_2 dominated planets to contract and eventually collapse in high opacity regime. The simplest way to understand this result is to (1) realise that a gentle sedimentation of grains onto a planet brings in additional gravitational potential energy but not thermal or kinetic energy, so that the total energy of the cloud becomes more negative. (2) The reason for a surprising sensitivity of molecular pre-collapse planets to metals is the fact that the total energy of a polytropic cloud with index n (equation 9) with $n \to 3$ is very small compared to $GM_{\rm p}^2/R_{\rm p}$ (e.g., $(3-n)/(5-n) = 0.2$ for $n = 5/2$), so it takes only a little extra weight in metals to topple the planet over into the unstable H_2 dissociation regime.

The implications of our results for TD hypothesis and GI-born planets are potentially significant. First of all, metal loading makes it much more likely that these planets are able to contract and collapse despite a rapid inward migration. This may help to resolve the challenges to forming GI planets at short separations by migration of fragments born at separations $\sim$ 100 AU emphasised by Zhu et al. (2012) and Vazan & Helled (2012). Secondly, metal loading process may explain why giant planets are over-abundant in metals (e.g., Miller & Fortney 2011). Finally, TD/GI planet survival may be enhanced at high metallicities since the rates of pebble accretion are higher, making the planets collapse sooner, while planet migration rates are unlikely to depend on disc metallicity strongly. This may produce a positive giant planet frequency – host star metallicity correlation as needed to explain observations (Fischer & Valenti 2005). These issues will be addressed in a separate forthcoming publication where the disc-planet interaction is modelled in detail.

As discussed in the Introduction, low opacity in pre-collapse GI clumps may be another way to speed up the collapse (Helled & Bodenheimer 2011), but it is not clear if opacity in the clumps is indeed much smaller than the interstellar one. Dullemond & Dominik (2005) argued that grain aggregate fragmentation in higher speed collisions is required by observations of T Tauri stars to maintain a high abundance of small grains despite the simultaneous presence of grains as large as $\sim$ 1 cm in size. Furthermore, the low dust opacity picture would predict a very efficient formation of giant planets at low metallicities, which contradicts observations (Fischer & Valenti 2005).

We also found that the response of giant planets to metal loading is a strong function of their mass. More mas-

sive planets are less likely to be influenced by metal accretion since they cool much more rapidly than their lower mass cousins (see fig. 7). This gives us hope that there may be strong trends in predictions of the TD model with fragment's mass that could hopefully be used to contrast it with observations of exoplanets.

The main shortcomings of our numerical approach here are (i) the simplification in the EOS that neglects metals' contribution to the internal energy and pressure of the mix (see Appendix), and (ii) assuming a homogenous spreading of the grains inside the planet. Both of these are made in order to keep our treatment as transparent as possible and to enable a comparison to the analytical model developed in §5. Furthermore, preliminary results of simulations with a more complete EOS show that this only strengthens the tendency of the fragments to collapse due to metal loading because grain vaporisation must occur before the fragment collapses (as $T \gtrsim 2000$ K at that point), and this process takes extra energy from the gas due to the latent heat of vaporisation (e.g., Podolak et al. 1988), cooling the fragment yet more. The assumption that grains are well mixed with gas is reasonable if convection stirs the grains up quickly (e.g., Helled & Bodenheimer 2011), mixing newly accreted grains throughout the planet efficiently. Nevertheless, we shall endeavour to relax these simplifications in future publications.

9 ACKNOWLEDGMENTS

Theoretical astrophysics research at the University of Leicester is supported by a STFC Rolling grant. The author thanks Richard Alexander for useful discussions.

REFERENCES

Baruteau C., Meru F., Paardekooper S.-J., 2011, MNRAS, 416, 1971
Blum J., Wurm G., 2008, ARA&A, 46, 21
Bodenheimer P., 1974, Icarus, 23, 319
Bodenheimer P., Grossman A. S., Decampli W. M., Marcy G., Pollack J. B., 1980, ICARUS, 41, 293
Bodenheimer P., Laughlin G. P., Rózyczka M., Yorke H. W., eds., 2007, Numerical Methods in Astrophysics: An Introduction
Boley A. C., 2009, ApJL, 695, L53
Boley A. C., Hartquist T. W., Durisen R. H., Michael S., 2007, ApJL, 656, L89
Boley A. C., Hayfield T., Mayer L., Durisen R. H., 2010, Icarus, 207, 509
Boley A. C., Helled R., Payne M. J., 2011, ArXiv e-prints
Boss A. P., 1997, Science, 276, 1836
Boss A. P., 1998, ApJ, 503, 923
Cameron A. G. W., Decampli W. M., Bodenheimer P., 1982, Icarus, 49, 298
Chandrasekhar S., 1957, An introduction to the study of stellar structure.
Dullemond C. P., Dominik C., 2005, A&A, 434, 971
Durisen R. H., Boss A. P., Mayer L., Nelson A. F., Quinn T., Rice W. K. M., 2007, Protostars and Planets V, 607–622
Fischer D. A., Valenti J., 2005, ApJ, 622, 1102
Forgan D., Rice K., 2011, MNRAS, 417, 1928
Forgan D., Rice K., 2013, MNRAS, 432, 3168
Gammie C. F., 2001, ApJ, 553, 174
Goldreich P., Tremaine S., 1980, ApJ, 241, 425
Helled R., Bodenheimer P., 2010, ICARUS, 207, 503
Helled R., Bodenheimer P., 2011, ICARUS, 211, 939
Helled R., Bodenheimer P., 2014, ApJ, 789, 69
Helled R., Podolak M., Kovetz A., 2008, Icarus, 195, 863
Helled R., Schubert G., 2008, Icarus, 198, 156
Hori Y., Ikoma M., 2011, MNRAS, 416, 1419
Johansen A., Lacerda P., 2010, MNRAS, 404, 475
Kuiper G. P., 1951, in 50th Anniversary of the Yerkes Observatory and Half a Century of Progress in Astrophysics, edited by J. A. Hynek, 357–+
Lambrechts M., Johansen A., 2012, A&A, 544, A32
Lambrechts M., Johansen A., 2014, ArXiv e-prints
Larson R. B., 1969, MNRAS, 145, 271
Lin D. N. C., Papaloizou J., 1979, MNRAS, 186, 799
Mayer L., Quinn T., Wadsley J., Stadel J., 2004, ApJ, 609, 1045
Mayor M., Queloz D., 1995, Nature, 378, 355
McCrea W. H., Williams I. P., 1965, Royal Society of London Proceedings Series A, 287, 143
Meru F., Bate M. R., 2011, MNRAS, 410, 559
Miller N., Fortney J. J., 2011, ApJL, 736, L29
Mizuno H., 1980, Progress of Theoretical Physics, 64, 544
Nayakshin S., 2010a, MNRAS, 408, L36
Nayakshin S., 2010b, MNRAS, 408, 2381
Nayakshin S., 2011a, MNRAS, 413, 1462
Nayakshin S., 2011b, MNRAS, 416, 2974
Nayakshin S., 2014, MNRAS, 441, 1380
Nayakshin S., Cha S.-H., 2013, MNRAS, 435, 2099
Nayakshin S., Helled R., Boley A. C., 2014, ArXiv e-prints
Nayakshin S., Lodato G., 2012, MNRAS, 426, 70
Ormel C. W., Klahr H. H., 2010, A&A, 520, A43
Podolak M., Pollack J. B., Reynolds R. T., 1988, ICARUS, 73, 163
Rafikov R. R., 2005, ApJL, 621, L69
Rice W. K. M., Lodato G., Armitage P. J., 2005, MNRAS, 364, L56
Stamatellos D., Whitworth A. P., 2008, A&A, 480, 879
Stevenson D. J., 1982, P&SS, 30, 755
Tsukamoto Y., Takahashi S. Z., Machida M. N., Inutsuka S.-i., 2014, ArXiv e-prints
Vazan A., Helled R., 2012, ApJ, 756, 90
Vazan A., Kovetz A., Podolak M., Helled R., 2013, MNRAS, 434, 3283
Wang J., Fischer D. A., 2013, ArXiv e-prints
Zhu Z., Hartmann L., Gammie C., 2009, ApJ, 694, 1045
Zhu Z., Hartmann L., Nelson R. P., Gammie C. F., 2012, ApJ, 746, 110

APPENDIX A: EQUATIONS

The equations are solved in spherical symmetry, with *gas* mass $M_{\rm g}$, the primary coordinate counted from the centre of the planet, used to set a staggered grid. The numerical time integration procedure is based on the Lagrangian scheme "lh1" presented in §6.2 of Bodenheimer et al. (2007). In the

one-fluid limit the equations are

$$\frac{1}{\rho} = 4\pi r^2 \frac{dr}{dM} \tag{A1}$$

$$\frac{dv}{dt} = -4\pi r^2 \frac{\partial P}{\partial M} - \frac{GM(r)}{r^2} \ , \tag{A2}$$

$$\frac{du}{dt} = -4\pi P \frac{\partial (r^2 v)}{\partial M} - 4\pi \frac{\partial \left(r^2 F(r)\right)}{\partial M} \tag{A3}$$

where $v = dr/dt$ is gas velocity, $M(r) = M_{\rm g}(r) + M_{\rm z}(r)$ is the total (gas + grains) mass enclosed within radius r, ρ and P is the total gas density and pressure at radius r. Note that since $1-z$ is the mass fraction of gas (H/He in the context of this paper), the total mass can be written as

$$M(r) = \frac{M_{\rm g}(r)}{1-z} \ , \tag{A4}$$

and similarly, total density $\rho = \rho_{\rm g}/(1-z)$ at all radii inside the planet. F is the radial energy flux, and is equal to either the radiative flux, $F_{\rm rad}$, given by the classical radiation flux,

$$F_{\rm rad} = -\frac{4 a_{\rm rad} c T^3}{3\kappa(T)} 4\pi r^2 \frac{\partial T}{\partial M} \ , \tag{A5}$$

where $a_{\rm rad}$ is the radiation constant, or $F_{\rm cov}$, the convective energy flux if the conditions for convective instability are satisfied. The latter is modelled according to the mixing length theory. The numerical scheme is explicit, with the time step limited by the Courant condition. An artificial viscosity is used to capture shocks. The equation of state (EOS) that we use provides gas pressure and internal energy as a function of total density $\rho_{\rm tot}$, metallicity z and gas temperature T. Since gas temperature T is not explicitly present in equations A1 to A3, at the end of each time step, which yields the values of P, ρ, u and z, at every mass zone, an iterative procedure is implemented to find the corresponding T.

The EOS of H/He mix with astrophysical metals is in general very complicated, and one needs an extensive chemical network to follow phase transitions and interactions between different chemical species. For example, Hori & Ikoma (2011) considered a number of compounds formed by elements C and O with hydrogen, and found that thermodynamical properties of gas change strongly at high metallicity ($z \to 1$). Vazan et al. (2013) used SiO_2 to model "rock" in their EOS. Lacking such proprietary EOS tables, we use a simpler approximation in which grains/metals do *not* contribute to the gas pressure or the internal energy of the gas other than by increasing the mass of the mixture. This approximation is excellent while metals are all in the grain phase because the energy in Brownian motion of the grains is negligible compared with that of the much lighter H/He molecules or atoms. The approximation is less well justified when grains are vaporised and the constituent molecules are broken down at higher temperatures. However, including the latent heat of grain vaporisation and metal molecules dissociation would only strengthen conclusions of our paper since the extra heat required for these processes would have been taken from the thermal energy of the fragment and would thus lead to its faster collapse. The simplified EOS we use therefore presents the minimum metal loading effect, and the more complicated forms of it must make it even stronger.

The H/He part of the EOS are modelled as that of an ideal H/He gas mixture which includes hydrogen molecules rotational and vibrational degrees of freedom (calculated as in Boley et al. 2007), and H_2 dissociation (cf. more technical detail in Nayakshin 2011b), as well as ionisation of hydrogen atoms. Ionisation of He atoms is not important for temperatures of interest, and is hence neglected.

The EOS of the toy model of an ideal polytropic gas planets that we use in §5 is $P = K\rho_{\rm tot}^{\gamma}$, where γ is a fixed adiabatic index, and K is a constant related to the entropy of the gas. The internal energy is then given by

$$u = \frac{P}{\rho} \frac{1}{\gamma - 1} \ . \tag{A6}$$

The mean molecular weight of the mixture is calculated as

$$\frac{1}{\mu} = \frac{1-z}{\mu_{\rm g}} + \frac{z}{\mu_{\rm dust}} = \frac{1-z}{\mu_{\rm g}} \ , \tag{A7}$$

where $\mu_{\rm g}$ is the mean molecular weight of the H/He mixture (which depends on the fraction of H atoms in H_2 molecules, atomic H and ionised H; He atoms are assumed to be not ionised). The last step in equation A7 is possible because the mean molecular weight of dust particles is orders of magnitude larger than $\mu_{\rm g}$.